Adsorption isotherms, kinetics and thermodynamics of NH_4^+–N from aqueous solutions using modified ceramsite and its regeneration performance

Tianpeng Li[a,b], Tingting Sun[c], Tallal Bin Aftab[a], Dengxin Li[a,*]

[a]*College of Environment Science and Engineering, Donghua University, Shanghai 201620, China, Tel. +86 2167792541;*
Fax: +86 2167792522; emails: lidengxin@dhu.edu.cn (D. Li), tianpeng985@126.com (T. Li), Tel. +86 13122174017;
email: tallal@live.com (T.B. Aftab)
[b]*College of City and Architecture Engineering, Zaozhuang University, Zaozhuang, Shandong 277160, China*
[c]*School of Basic Medical Science, Wenzhou Medical University, Wenzhou, Zhejiang 325035, China, Tel. +86 57188208160;*
email: ttsun@zju.edu.cn

ABSTRACT

Ceramsite was prepared from solid wastes by high-temperature sintering process and modified using NaCl solution. The adsorption of ammonium nitrogen (NH_4^+–N) from aqueous solution by modified ceramsite (MC) and its chlorination regeneration were investigated. The results showed that the q_e of MC was 2.49 mg/g after being stirred for 180 min when initial concentration of NH_4^+–N was 100 mg/L at 328 K, which was 1.79 times higher than that of ceramsite. The adsorption process of NH_4^+–N on MC can be well described by the Langmuir isotherm model in the whole experiments, with $R^2 > 0.95$ and root mean squared error (RMSE) < 0.02. On the contrary, the adsorption process of NH_4^+–N on ceramsite followed the Freundlich isotherm model, with $R^2 > 0.95$. Compared with the pseudo-second-order reaction kinetics, the adsorption of NH_4^+–N onto MC fitted better in the pseudo-first-order reaction kinetics when initial concentration of NH_4^+–N was 35 mg/L at 298 K, with $R^2 > 0.95$, standard deviation error <0.13 and RMSE <0.13. The thermodynamics results indicated that the adsorption process of NH_4^+–N onto MC was a spontaneous, endothermic and physisorption process. Moreover, the regeneration results demonstrated that NaClO solution was an effective regenerant for the recovery of exhausted MC, the q_e of MC was about 1.50 mg/g even after 15 cycles and no significant change compared with initial.

Keywords: Ceramsite; Modification; Adsorption capacity; Physisorption process; Chlorination

1. Introduction

Nitrogen element is essential for nucleic acid and protein synthesis, the two most important polymers of life, and its compounds are nutrients essential to all forms of life. Generally, NH_4^+–N is one of the main forms of nitrogen compounds encountered in aquatic environment [1]. The presence of excessive amounts of NH_4^+–N or its compounds in water bodies causes serious ecological and environmental backlashes. The most representative environmental problem is water eutrophication [2], resulting in excessive growth of algae and other microorganisms in lakes and rivers, depletion of dissolved oxygen and toxicity in aquatic fauna. Nowadays, with the increasing awareness of the deleterious and detrimental effects of NH_4^+–N, many developed and developing countries have enlarged pollution control of NH_4^+–N, and drew up the stricter discharge standard for NH_4^+–N. For example, in China, the discharge standard of NH_4^+–N has been established (Discharge Standard of Pollutants for Municipal Wastewater Treatment Plant, GB 18918-2002), and it was set to 5.0 and 8.0 mg/L for A and B standard of I grade

* Corresponding author.

effluent, respectively. Therefore, it is obligatory and very important to remove NH_4^+–N from wastewater prior to discharge.

Currently, various technologies have been employed to treat NH_4^+–N wastewater, such as biological and hybrid methods, including microalgae *Scenedesmus* sp. [3], biological aerated filter [4] and combine anammox with partial denitrification [5]; physical–chemical and their combined processes, including air stripping [6], electrodialysis [7], chlorination decomposition [8], hollow-fiber membrane contactors [9], chemical precipitation recycle technology [10] and other methods [11,12]. Compared with the abovementioned technologies, adsorption is considered as a reliable and effective technique, mainly due to its high efficiency, low-cost, easy operation and avoidance of chemical sludge [13–15]. It was reported that several alternative adsorbents, such as natural zeolite [16], modified Ca-bentonites [17] and Fe_3O_4 nanoparticles [18], have been applied for NH_4^+–N wastewater treatment. Unfortunately, there are still some shortcomings for practical application of the above adsorbents. For instance, bentonites and natural zeolite belong to mineral resources, which do not meet with the requirements of sustainable development. Meanwhile, considering rigorous ecological and commercial demands for sustainability, repeated reuse of adsorbents is one of the most important parameters for routine applications [19,20]. Hence, it is critical to continue investigating on alternative cheaper adsorbents as these adsorption materials are unsustainable or nonreusable.

Ceramsite, with high porosity, large specific surface area, low bulk, apparent density and less toxic, has been used as building materials [21], as well as filter media or adsorption material in water treatment [22]. Traditionally, natural resources were used as main raw materials to prepare ceramsite, such as shale and clay [23]. A review literature summarized, two important development trends of ceramsite in recent years. On the one hand, more and more solid wastes, including dewatered sewage sludge (DSS), river or marine sediment, coal fly ash (CFA), construction and demolition and glass cullet, were selected as a potential substitute to replace natural resources for production of ceramsite [24,25], which may provide a prospective pathway for municipal wastes utilization [26]. On the other hand, the surface functional group of ceramsite was modified by oxides or hydroxides, such as pure magnetite Fe_3O_4 [27], nanotitanium dioxide (TiO_2) [28] and fusion with sodium hydroxide (NaOH) [29], in order to improve the treatment efficiency or extend the application scope. In this study, ceramsite was obtained from DSS, CFA and river sediment, without using any natural resources, pursuing the concept of sustainable development. And then, it was used to treat wastewater having NH_4^+–N after modification and characterization, providing a prospective pathway for solid wastes utilization [30].

The primary objectives of this research were as follows: first, ceramsite, obtained from solid wastes, was prepared by high-temperature sintering process. Second, ceramsite was characterized before/after modification. Third, the adsorption of NH_4^+–N from aqueous solutions using MC was carried out. Finally, the regeneration performance of exhausted MC was analyzed.

2. Experimental

2.1. Materials and reagents

Ceramsite (about 10 mm diameter) used in this research from DSS (Shanghai Songjiang Sewage Treatment Plant, China), CFA (Shanghai Waigaoqiao Power Generation Co. Ltd., China) and river sediment (Songjiang Campus of Donghua University, China), which was prepared by a high-temperature sintering process. The results of the composition of raw materials, preparation process, physical properties and heavy metal leaching toxicity of ceramsite were all detailed in our previous researches [31–33]. In brief, the physical properties of ceramsite, included breaking and wear rate (0.2%), solubility in hydrochloric acid (0.01%), silt carrying capacity (0.2%), void fraction (71.1%) and S_{BET} (0.75×10^4 cm^2/g), met with the China's industrial standard of Artificial Ceramsite Filter Material for Water Treatment (CJ/T 299-2008). The concentration of heavy metals in the lixivium of ceramsite was lower than the national thresholds of Identification Standards for Hazardous Wastes-Identification for Extraction Toxicity (GB 5085.3-2007). Therefore, we can draw a conclusion that the lab made ceramsite has a promising application for using as filter media, adsorbent or other media/materials in water treatment, and is in well agreement with the results of other researches [34,35].

Ammonium chloride (NH_4Cl), sodium chloride (NaCl) and sodium hypochlorite (NaClO) were purchased from Sinopharm Chemical Reagent Co. Ltd., China. All chemical reagents appeared in this study were of analytical grade and were used as received without further purification. Deionized water was applied for all the experiments.

2.2. Modification tests

Before modification, ceramsite was crushed down and sieved to a diameter of about 1.0 ± 0.1 mm, and washed with deionized water to remove the water-soluble residues and other undesirable materials, and then dried in a drying oven at 105°C for over 4 h.

The chemical compositions of ceramsite were similar with natural zeolite, such as SiO_2, Al_2O_3, Fe_2O_3, CaO and MgO [36]. In addition, the physical properties, such as S_{BET}, void fraction and apparent density of ceramsite were also same as natural zeolite. Therefore, ceramsite was modified using NaCl solution according to the modification method of natural zeolite [37]. The modification conditions adopted in this experiment were as follows: 1 mol/L of NaCl solution, stirring time of 60 min (120 rpm), a temperature of 80°C and ceramsite/NaCl solution ratio maintained as 1 g:10 mL. Afterwards, the samples were rinsed with deionized water and dried in a thermostatic drum wind drying oven at 105°C for about 180 min.

2.3. Batch experiments

1,000 mg/L of NH_4^+–N stock solution was obtained by dissolving 3.819 g of NH_4Cl in 1,000 mL deionized water. 100 mL of simulated NH_4^+–N wastewater with different initial concentrations in the range of 20–100 mg/L were prepared by stepwise dilution of the stock solution. The experimental procedure followed was as below: a 250 mL

breaker was placed on a magnetic stirrer (120 rpm) and into which 100 mL NH_4^+–N wastewater was first poured, and 2.0 g absorbent was added to the solution. At given temperature and time intervals, the concentration of NH_4^+–N in the effluent was examined. All of the experiments under the same conditions were performed in triplicate.

2.4. Analysis

The samples were characterized by a variety of techniques, such as a scanning electron microscope–energy dispersive spectrometer (SEM–EDS; Quanta-250, Fei Instrument, Czech Republic) was used to observe the surface morphology of samples with an accelerating voltage of 13 kV, the surface of samples was sputtered with gold layer in order to improve the quality of the images. The Brunauer–Emmett–Teller (BET) specific surface area (S_{BET}), total pore volume and average pore size were calculated from N_2 adsorption and desorption measurements obtained using fully automatic specific and micropore size analyzer (AUTOSORB-IQ2-MP, USA). Fourier transform infrared spectrophotometer (FTIR; Bruker Tensor 27, Germany) was employed to study the chemical structures of samples, FTIR spectra were taken on a KBr disk at a frequency range of 4,000–400 cm^{-1}. The concentrations of NH_4^+–N in the effluent were detected using Nessler's reagent (HgI_2–KI–NaOH) spectrophotometrically at a wavelength of 420 nm according to the industrial standard of China (HJ 535-2009). The adsorption capacity at t min (q_t, mg/g) and adsorption capacity at equilibrium (q_e, mg/g) were calculated according to Eqs. (1) and (2) [38], respectively.

$$q_t = \frac{(C_0 - C_t)V}{m} \tag{1}$$

$$q_e = \frac{(C_0 - C_e)V}{m} \tag{2}$$

where C_0 and C_e are the initial concentration and equilibrium concentration of NH_4^+–N, respectively, mg/L. V is the volume of the working simulated wastewater, L. m is the mass of added adsorbent, g.

3. Results and discussion

3.1. Characterization

3.1.1. SEM–EDS study

As illustrated in Fig. 1(a), the ceramsite has a lot of ravines, pore channels crossing, uneven size, as well as quite smooth and highly polished surface. Comparably, Fig. 1(b) reflected that the surface of MC is rough, porous and less smooth. The EDS spectra indicated that before and after modification, the content of Na element in the surface of ceramsite increased from 2.85 to 6.18 (wt%), being doubled (Figs. 1(a) and (b)). The results suggested that the functional group (Na^+) was grafted on the surface or on the pores of ceramsite after modification.

3.1.2. BET study

A typical N_2 adsorption–desorption isotherms of samples were investigated, and the results were presented in Fig. 2.
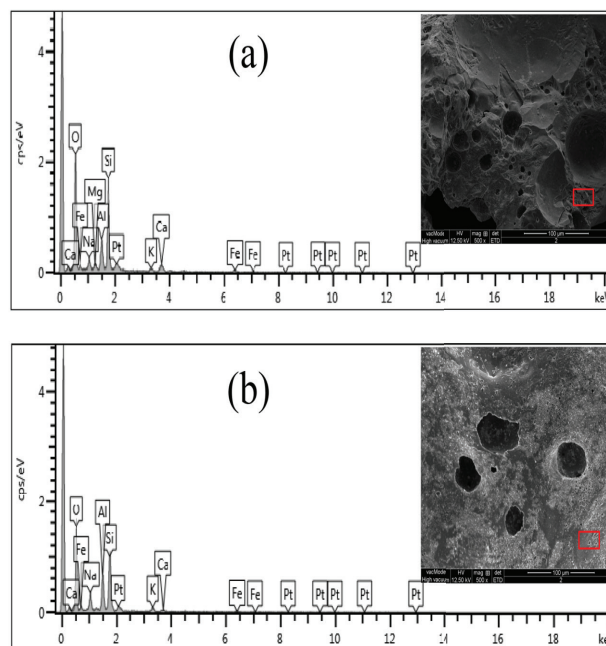

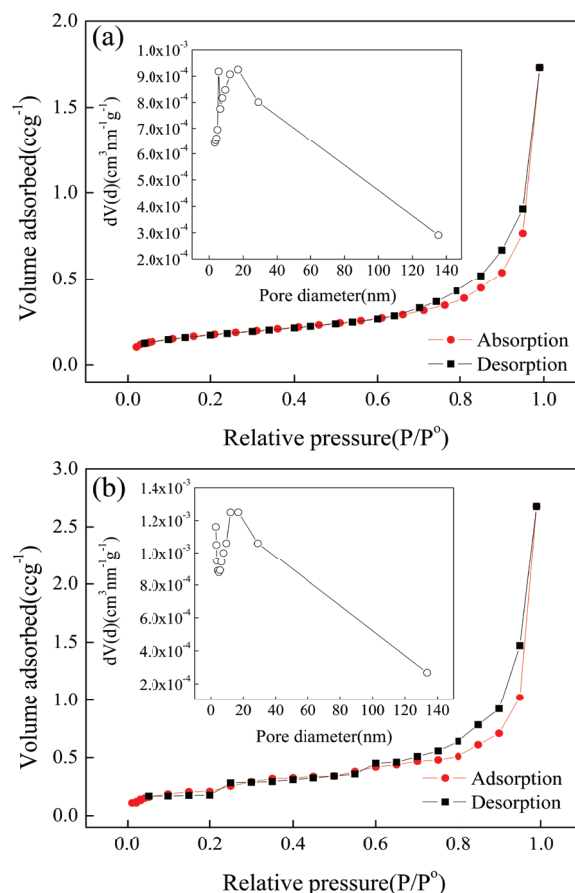Fig. 1. SEM images and EDS spectra of (a) ceramsite and (b) MC.

Fig. 2. N_2 adsorption–desorption isotherms and pore-size distribution (inset) of (a) ceramsite and (b) MC.

It was found that both of the two samples showed type IV isotherms with hysteresis loop at P/P_0 = 0.45–0.95, and the isotherms showed high absorption at high relative pressure P/P_0 = 0.99. The S_{BET}, total pore volume and average pore size of the ceramsite were measured to be 0.63 m²/g, 0.091 cm³/g and 118.9 nm, respectively (Fig. 2(a)). Similarly, the S_{BET}, total pore volume and average pore size of the MC were measured to be 0.798 m²/g, 0.086 cm³/g and 166.1 nm, respectively (Fig. 2(b)). It was suggested that the S_{BET} and average pore size of MC are 1.23 and 1.4 times more than that of ceramsite. Fig. 1(b) illustrated that the decrease in total pore volume may be due to the functional group (Na⁺) deposition.

3.1.3. FTIR study

As shown in Fig. 3, the FTIR spectra results revealed that there were great similarities between the ceramsite and MC, the weak peaks appeared approximately at 501, 632, 1,271 and 1,452 cm⁻¹, mainly because of out-of-plane rocking vibration of O–C–O, bending vibration of C–O–H and stretching vibration of C=O [39,40]. Remarkably, the FTIR spectrum of ceramsite appeared a significantly characteristic peak at 3,417.78173 cm⁻¹ (Fig. 3(a)), may be owing to the hydroxyl (–OH) stretching vibration [41]. By contrast, the FTIR spectrum of MC of this characteristic peak at 3,417.78173 cm⁻¹ became much narrower (Fig. 3(b)), probably due to the fact that the hydrogen element on the –OH was replaced by Na⁺ and the process can be expressed by Eq. (3).

$$-OH + Na^+ \Leftrightarrow -ONa + H^+ \tag{3}$$

3.2. Adsorption isotherms

In order to evaluate the optimal adsorbent for NH_4^+–N from aqueous solution, the equilibrium isotherms of ceramsite and MC were studied under different reaction temperatures and initial concentrations, and the results are displayed in Fig. 4. Fig. 4(b) shows the q_e of ceramsite increased with the increasing of initial concentrations and temperatures. When initial concentrations increased
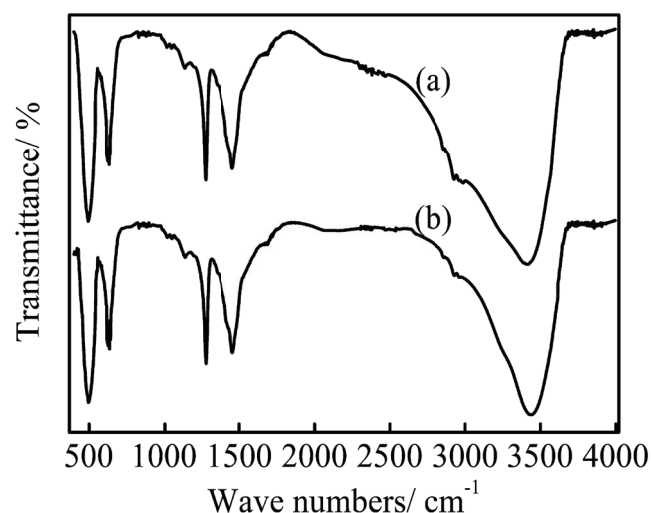
from 20 to 100 mg/L and temperatures increased from 298 to 328 K, the q_e of ceramsite increased 63.47% after being stirred for 180 min. These can be interpreted as the following two aspects: one is that the unique physical properties, pore characteristics and surface morphology of ceramsite, which does not adsorb nitrogen and phosphorus directly [42], but other important parameters that have remarkable positive correlation with cation exchange capacity [43]. The other is that for the same unit mass exchange site, a higher initial concentration resulted in a stronger driving force generating from the higher concentration gradient and then conduce higher adsorption capacity [44].

Fig. 4(a) indicated that after being stirred for 180 min, the q_e of MC increased from 0.87 mg/g at initial concentration of 20 mg/L and 298 K, to the maximum value of 2.49 mg/g when initial concentration was 100 mg/L and 328 K, increased about 2.9 times. Compared with Figs. 4(a) and (b), the q_e of MC was much higher than that of ceramsite after being stirred for 180 min at the same experimental conditions. For example, at the initial concentration of 35 mg/L and 298 K, the q_e of MC was 1.29 mg/g, which was about 51.67% higher than that of ceramsite. The results determined that the q_e of ceramsite for NH_4^+–N has been obviously enhanced at the initial concentrations ranges between 20 and 100 mg/L, implying that the modification method was successful for improving the adsorption capacity of ceramsite. This attributes to the S_{BET}
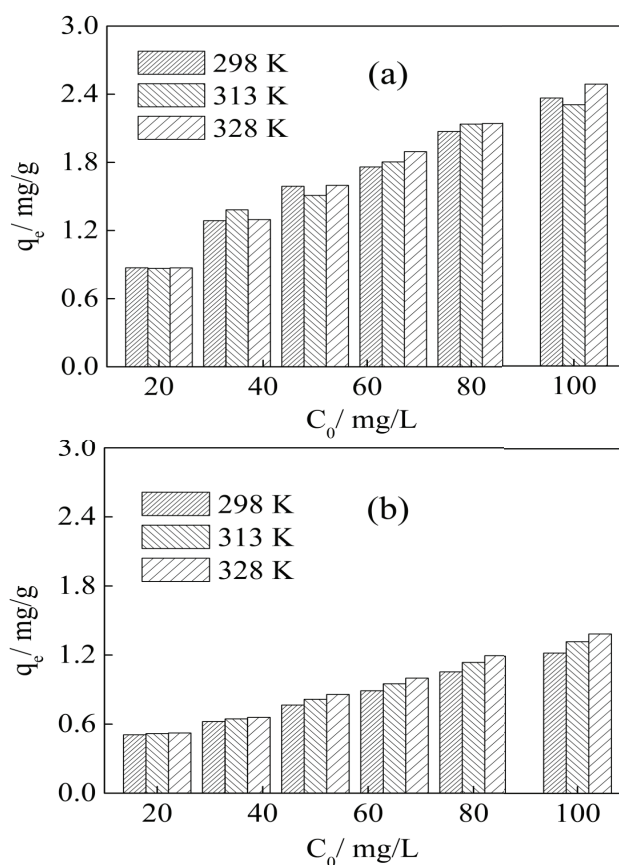
Fig. 4. Equilibrium isotherm data for NH_4^+–N adsorption on (a) MC and (b) ceramsite after being stirred for 180 min.

Fig. 3. FTIR spectra of (a) ceramsite and (b) MC.

and average pore size of MC were much larger than that of ceramsite (Fig. 2), emphasizing that the MC could remove selectively NH_4^+–N ion. Additionally, according to the EDS spectra (Fig. 1) and Eq. (3), determining that the ion-exchange reaction should be one of the main mechanisms for the removal of NH_4^+–N from aqueous solutions by MC, which can be expressed by Eq. (4).

$$Ceramsite - Na + NH_4^+ \Leftrightarrow Ceramsite - NH_4 + Na^+ \qquad (4)$$
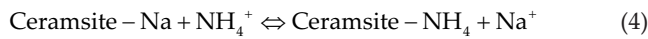
As the ion-exchange reaction proceeded, the concentrations of Na^+ and NH_4^+ in the solution increased and decreased, respectively. As a consequence, the driving force of NH_4^+ ion-exchange onto the ceramsite decreased. Besides, comparison of equilibrium adsorption capacity of NH_4^+–N on various adsorbents under different reaction temperatures were summarized (Table 1). As the table presented, the q_e value of MC in this work was better than those mentioned adsorbents, suggesting that the lab made MC exhibits a promising efficiency to remove NH_4^+–N from aqueous solutions.

Usually, equilibrium data, known as adsorption isotherms, are important in the basic design of adsorption systems, and are critical in optimizing the use of adsorbents. Hence, the most appropriate correlation coefficient (R^2) for the equilibrium curves should be established, optimizing the design of an adsorption equilibrium system in the removal of NH_4^+–N from aqueous solutions. Furthermore, in order to comprehensive provenience the fit quality of the relative models involved, the mean error (ME), standard deviation error (SDE) and RMSE were developed, and their evaluation indexes were defined by Eqs. (5)–(7) [45], respectively.

$$ME = \frac{1}{n}\sum_{i=1}^{n}(x_{i1} - x_{i2}) \qquad (5)$$

$$SDE = \sqrt{\frac{1}{n-1}\sum_{i=1}^{n}\left[(x_{i1} - x_{i2}) - ME\right]^2} \qquad (6)$$

$$RMSE = \sqrt{\frac{1}{n}\sum_{i=1}^{n}(x_{i1} - x_{i2})^2} \qquad (7)$$

where x_{i1} and x_{i2} are the measured value and prediction value of NH_4^+–N of the ith sample, respectively. n is the total number of observations.

The Langmuir and Freundlich isotherm models are commonly used for explaining monolayer homogeneous adsorption processes and modeling the adsorption on heterogeneous surfaces, respectively [46]. Thus, both Langmuir and Freundlich isotherm models were selected to analyze the experimental results, and their linear isotherm equations are expressed by Eqs. (8) and (9), respectively.

$$\frac{C_e}{q_e} = \frac{1}{q_m K_L} + \frac{C_e}{q_m} \qquad (8)$$

$$\ln q_e = \ln K_F + \frac{1}{n}\ln C_e \qquad (9)$$

where q_m is the maximum adsorption capacity, mg/g. $1/n$ is the heterogeneity factor, ranges between 0 and 1. K_L (L/mg) and K_F ((mg/g)(L/mg)$^{1/n}$) are the Langmuir and Freundlich isotherm constants, respectively.

Based on Eqs. (8) and (9), the linear plots of Langmuir and Freundlich isotherms of NH_4^+–N adsorption on adsorbents are detailed in Figs. 5 and 6. The values of q_m, K_L, K_F, n, R^2, SDE and RMSE were calculated from the slope of curves in Figs. 5 and 6 at 298, 313 and 328 K, respectively, and the results are listed in Table 2. Fig. 5(a) and Table 2 demonstrate the adsorption equilibrium of NH_4^+–N on MC can be well described by the Langmuir isotherm model in the investigated reaction temperatures, with high R^2 values (more than 0.96) and low SDE and RMSE values (less than 0.13 and 0.02, respectively). Fig. 6(a) and Table 2 suggest the Freundlich isotherm model can also adequately describe the equilibrium of NH_4^+–N adsorption on MC, judging only from $R^2 > 0.95$. These results confirmed that the adsorption of NH_4^+–N on MC was a monolayer homogeneous adsorption processes. In addition, the adsorption of NH_4^+–N occurred on the heterogeneous surface of MC.

Fig. 5(b) and Table 2 indicate the Langmuir isotherm model unsuitably described the adsorption equilibrium of NH_4^+–N on ceramsite in this experimental conditions, owing to the values of R^2 were less than 0.93, and more importantly, the values of SDE and RMSE were more than 0.27 and 0.02, respectively. We can infer that the adsorption of NH_4^+–N on ceramsite could not be a monolayer homogeneous adsorption processes, but a multilayer homogeneous or multilayer heterogeneous adsorption processes. Fig. 6(b) and Table 2 display the equilibrium of NH_4^+–N adsorption on ceramsite could be well fitted with the Freundlich isotherm model, with the value of R^2 was more than 0.95, manifesting that NH_4^+–N can be adsorbed on the heterogeneous surface of ceramsite.

Table 1
Comparison of q_e (mg/g) of NH_4^+–N on various adsorbents

Adsorbents	Temperature (K)	q_e (mg/g)	References
Ceramsite	298	1.22	This study
MC	298	2.37	This study
Chitosan–bentonite film composite	Room temperature	≤1.0	[14]
Loose-pore geothermal reservoir	333	≤0.5	[15]
Ceramsite material	298	≤1.57	[42]
Natural Chinese (Chende) zeolite	300	2.89	[47]
Modified zeolite	Room temperature	2.01	[54]

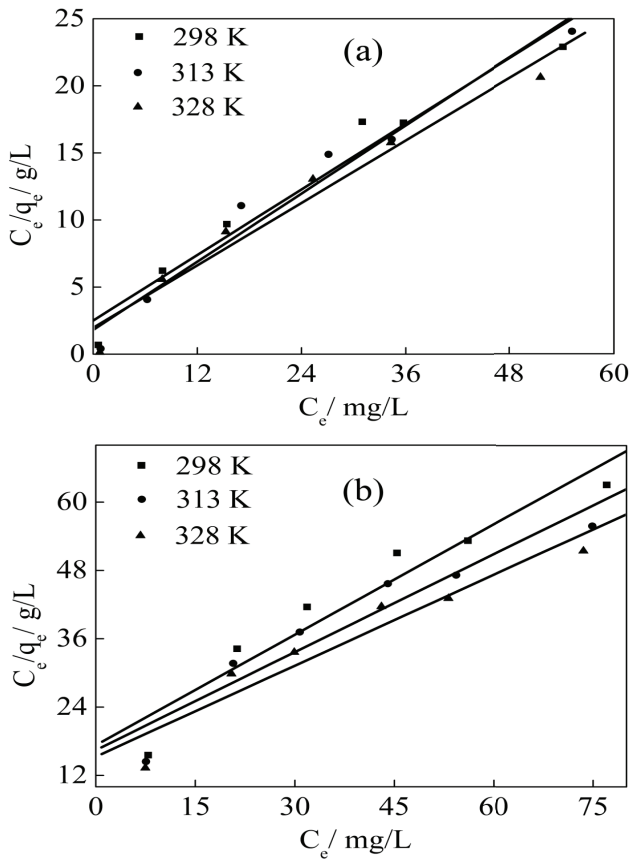Fig. 5. Linear plot of Langmuir isotherm of NH_4^+–N adsorption on (a) MC and (b) ceramsite.

Fig. 6. Linear plot of Freundlich isotherm of NH_4^+–N adsorption on (a) MC and (b) ceramsite.

Furthermore, the values of $1/n$ for both MC and ceramsite were always less than 1.0 throughout the experiments, demonstrating that the adsorption of NH_4^+–N on MC or ceramsite is operationally and economically very effective [47]. In conclusion, we choose the MC as the optimal adsorbent to investigate the effect of other factors on the removal of NH_4^+–N from aqueous solution.

3.3. Adsorption kinetics

To investigate the adsorption kinetics of MC for NH_4^+–N from aqueous solution, characteristic constants of adsorption were measured using pseudo-first-order and pseudo-second-order reaction kinetics [48]. The linear equations are represented by Eqs. (10) and (11) [18], respectively.

$$\ln(q_e - q_t) = \ln q_e - K_1 t \tag{10}$$

$$\frac{t}{q_t} = \frac{1}{K_2 q_e^2} + \left(\frac{1}{q_e}\right) t \tag{11}$$

where K_1 (g/min·mg) and K_2 (g/min·mg) are the rate constants of the pseudo-first-order and pseudo-second-order reaction kinetics, respectively.

The parameters, such as K_1, K_2, $q_{e,cal}$, R^2, SDE and RMSE, were calculated based on the kinetic plots of $\ln(q_e - q_t)$ and t/q_t vs. t, which are listed in Fig. 7 and Table 3 for varying
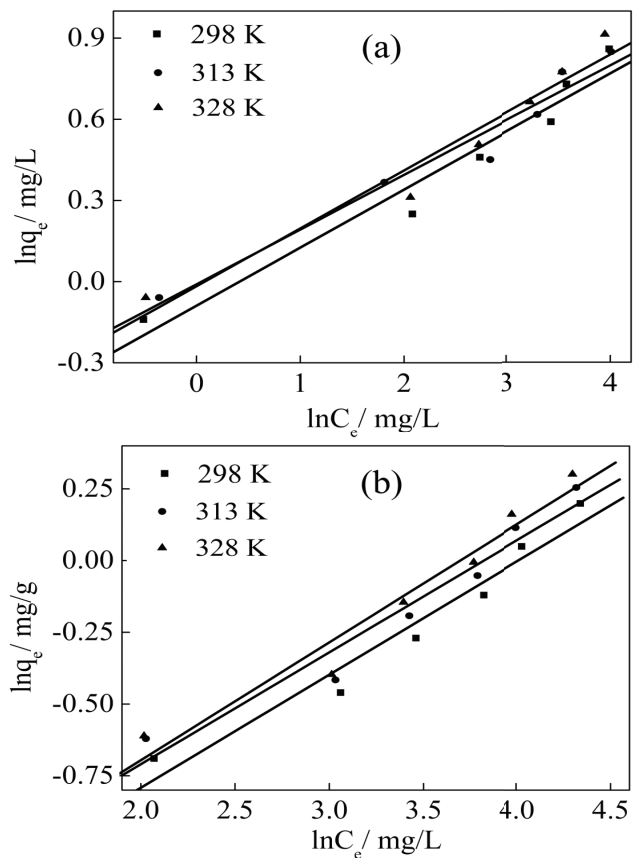
NH_4^+–N initial concentrations (from 35 to 65 mg/L) at 298 K. As seen from Fig. 7(a) and Table 3, the high R^2 (>0.95) and small SDE (<0.13) and RMSE (<0.12) were obtained in the investigated initial low-concentrations, which proving that the adsorption of NH_4^+–N on MC well followed the pseudo-first-order reaction kinetics. Besides, the value of R^2 descended with the increase of initial concentration. The results indicated that MC is more suitable for the treatment of low-concentration NH_4^+–N wastewater. As can be seen from Fig. 7(b) and Table 3, the values of R^2 were less than 0.95 in the investigated initial concentrations, which suggesting that the adsorption of NH_4^+–N on MC could not be well described by the pseudo-second-order reaction kinetics.

Additionally, the SDE values of pseudo-first-order reaction kinetics were higher than that of pseudo-second-order reaction kinetics. In the same way, the RMSE values of pseudo-first-order reaction kinetics were higher than that of pseudo-second-order reaction kinetics. It was demonstrated that the pseudo-first-order reaction kinetics illustrated better linear correlation and prediction accuracy than the pseudo-second-order reaction kinetics.

3.4. Adsorption thermodynamics

The thermodynamics parameters of NH_4^+–N adsorption on MC in various initial concentrations (35–65 mg/L) at

Table 2
Langmuir and Freundlich isotherm model constants and R^2 for adsorption of NH_4^+–N onto adsorbents at various temperatures

Adsorbents	Temperature (K)	Langmuir isotherm					Freundlich isotherm		
		q_m (mg/g)	K_L (L/mg)	R^2	SDE	RMSE	K_F (mg/g)(L/mg)$^{1/n}$	$1/n$	R^2
MC	298	2.455	0.163	0.962	0.073	0.0082	0.915	0.215	0.953
	313	2.422	0.183	0.969	0.096	0.0057	0.917	0.218	0.960
	328	2.644	0.147	0.963	0.129	0.016	0.91	0.231	0.954
Ceramsite	298	1.547	0.0374	0.925	0.266	0.017	0.206	0.394	0.955
	313	1.724	0.0344	0.915	0.329	0.082	0.201	0.421	0.950
	328	1.856	0.0328	0.914	0.382	0.122	0.196	0.443	0.955

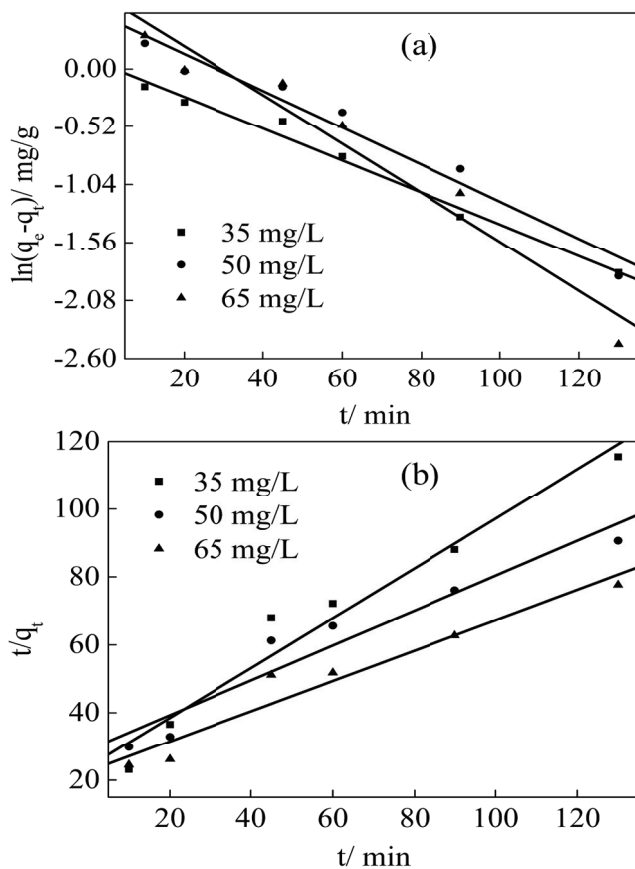
Fig. 7. (a) Pseudo-first-order reaction kinetics and (b) pseudo-second-order reaction kinetics for NH_4^+–N adsorption onto MC from aqueous solution.

298 K, involves the standard Gibbs free energy changes ($\Delta G°$, kJ/mol), standard enthalpy change ($\Delta H°$, kJ/mol) and standard entropy change ($\Delta S°$, kJ/mol) were calculated using the following equations [49,50]:

$$K_D = \frac{C_0 - C_e}{C_e} \times \frac{V}{m} \qquad (12)$$
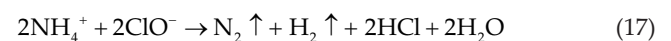
$$\Delta G° = -RT \ln K_D \qquad (13)$$

$$\Delta G° = \Delta H° - T \cdot \Delta S° \qquad (14)$$

where R is the universal gas constant, 8.314 J/mol·K. T is the absolute solution temperature, K. K_D is the solid–liquid partition coefficient, mL/g.

First, the values of K_D under different initial concentrations (35, 50 and 65 mg/L) were calculated according to Eq. (12). Subsequently, the values of $\Delta G°$ were obtained according to Eq. (13). Finally, the values of $\Delta H°$ and $\Delta S°$ were calculated according to Eq. (14), and the results were presented in Table 4. The results showed that $\Delta G°$ values were less than 0.0 kJ/mol in all initial concentrations, generally determining that NH_4^+–N adsorption on MC was favorable and spontaneous. Additionally, the $\Delta G°$ changes in the range of –20.0 to 0.0 kJ/mol, further demonstrating that NH_4^+–N adsorption on MC was a physisorption process [51]. The positive values of $\Delta H°$ confirmed that the adsorption process of NH_4^+–N using MC was endothermic reaction, adequate raise in temperature will be helpful for the adsorption. Positive $\Delta S°$ values demonstrated that the adsorption process of NH_4^+–N by MC was a process of entropy increase, the increased randomness and affinity in adsorption of NH_4^+–N on MC at the solid/solution interface will be established.

3.5. Regeneration performance

For real applications, the reusability and reproducibility is a very important and crucial factor to obtain an advanced and efficient adsorbent, since it can be regenerated for next applications. An excellent adsorbent should not only possess high adsorption efficiency, but also exhibit strong regeneration capacity, which may significantly reduce the overall cost of adsorption process [52,53]. Herein, when the MC of adsorption NH_4^+–N saturated, it was collected and then regenerated by chlorination method, using NaClO solution as a regenerant. The regeneration method was as follows [54]: the Cl:N mass ratio of 8.0, pH of 7 and stirred for 90 min (120 rpm) at room temperature. The chlorination regeneration mechanisms can be expressed as:

$$NaClO \rightarrow Na^+ + ClO^- \qquad (15)$$

$$Ceramsite - NH_4 + Na^+ \Leftrightarrow Ceramsite - Na + NH_4^+ \qquad (16)$$

$$2NH_4^+ + 2ClO^- \rightarrow N_2 \uparrow + H_2 \uparrow + 2HCl + 2H_2O \qquad (17)$$

After regeneration, the samples were washed several times with deionized water and dried at 105°C for 180 min.

Table 3
Rate constants and R^2 for the studied kinetic models under different NH_4^+–N initial concentrations at 298 K

C_0 (mg/L)	$q_{e,exp}$ (mg/g)	Pseudo-first-order					Pseudo-second-order				
		$K_1 \times 10^{-2}$ (g/min mg)	$q_{e,cal}$ (mg/g)	R^2	SDE	RMSE	$K_2 \times 10^{-2}$ (g/min mg)	$q_{e,cal}$ (mg/g)	R^2	SDE	RMSE
35	1.287	3.29	1.41	0.985	0.126	0.100	2.26	1.36	0.949	0.0404	0.0596
50	1.589	3.82	1.59	0.963	0.00061	0.00082	0.91	1.95	0.929	0.332	0.295
65	1.759	5.07	1.91	0.952	0.111	0.123	0.89	2.24	0.943	0.448	0.393

Table 4
Thermodynamic parameters for NH_4^+–N adsorption on MC at various initial concentrations (298 K)

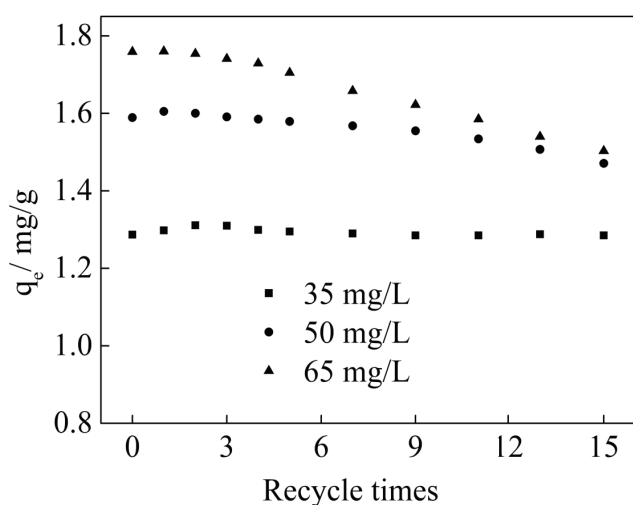| C_0 (mg/L)	Temperature (K)	$\ln K_D$ (mL/g)	$\Delta G°$ (kJ/mol)	$\Delta H° \times 10^{-1}$ (kJ/mol)	$\Delta S° \times 10^{-2}$ (kJ/mol)
35	298	5.08	–12.586	5.30	4.50
	313	5.42	–14.112		
	328	5.11	–13.935		
50	298	4.64	–11.486	6.52	4.00
	313	4.49	–11.674		
	328	4.66	–12.694		
65	298	3.95	–9.784	9.86	6.60
	313	4.20	–10.924		
	328	4.32	–11.767		

Fig. 8. The effect of recycle times on q_e (mg/g) of MC for NH_4^+–N from aqueous solution.

And then batch experiments were carried out using the regenerated MC at 298 K, according to the section batch experiments. The experimental results under the same conditions were measured in triplicate, and an averaged value was employed.

The effect of recycle times on equilibrium isotherms for NH_4^+–N uptake onto regenerated MC were discussed under different initial concentrations (35, 50 and 60 mg/L), and the results are illustrated in Fig. 8. It was demonstrated that no obvious deterioration tendency was appeared for the q_e of MC within 15 operational recycles when the initial concentration

was 35 mg/L and with the recycle time increased. The results also depict that the q_e of MC of regenerated from 1 to 15 recycle times was more than the original q_e of MC. The most possible reason is that ClO^- ions adsorbed on the surface of MC, can oxidize and remove NH_4^+–N. On the contrary, the q_e of MC declined by 7.43% and 14.55%, respectively after 15 recycle times when initial concentrations were 50 and 65 mg/L.

The decrease in the q_e of MC can be attributed to the facts that on the one side, the MC loss during the process of washing, which resulting in the experimental error. And on the other side, a portion of active groups, such as –OH and carboxyl (–COOH), were oxidized by ClO^- ion during regeneration process. The MC loss also reduced the available ion-exchange sites of ceramsite for Na^+, which resulting in the reduction of the adsorption capacity of ceramsite for NH_4^+–N. In addition, during regeneration process, the exchanged NH_4^+ ion into MC, was not completely released [55], weakening the ion-exchange ability of ceramsite and leading to its adsorption capacity decreased. Taken together, we can be concluded that although a slight decrease in q_e of MC for NH_4^+–N from aqueous solution was observed in the reuse process, the chlorination method might also be considered as an effective regeneration method for the exhausted MC.

4. Conclusions

The main conclusions extracted from this research can be summarized as follows:

- Compared with ceramsite, the q_e of MC has increased by about 1.8 times, confirming that 1 mol/L NaCl solution is a relatively perfect modifying agent, which can be used to modify ceramsite.

- The Langmuir and Freundlich isotherm models fitted the adsorption process of NH_4^+–N on MC, indicating that the adsorption process is a monolayer homogeneous adsorption process, and the adsorption occurred on the heterogeneous surface of MC.
- Compared with pseudo-second-order reaction kinetics, pseudo-first-order reaction kinetics were well described the adsorption of NH_4^+–N onto MC in all investigated initial concentrations, with higher R^2 values and smaller SDE and RMSE values. Besides, the adsorption process of NH_4^+–N on MC is a physisorption, spontaneous and entropy-driven process.
- Regeneration results showed that chlorination has proved to be an effective regeneration method for exhausted MC. The prominent advantage of this method is that regeneration process can run at the same time as modification is ongoing.

Acknowledgments

References

[1] A. Arslan, S. Veli, Zeolite 13X for adsorption of ammonium ions from aqueous solutions and hen slaughterhouse wastewaters, J. Taiwan Inst. Chem. Eng., 43 (2012) 393–398.

[2] B. Norddahla, V.G. Horna, M. Larsson, J.H.D. Preez, K. Christensen, A membrane contactor for ammonia stripping, pilot scale experience and modeling, Desalination, 199 (2006) 172–174.

[3] A. Ruiz-Martinez, J. Serralta, A. Seco, J. Ferrer, Effect of temperature on ammonium removal in *Scenedesmus* sp., Bioresour. Technol., 191 (2015) 346–349.

[4] W.S. Chang, H.T. Tran, D.H. Park, D.H. Aha, Ammonium nitrogen removal characteristics of zeolite media in a biological aerated filter (BAF) for the treatment of textile wastewater, J. Ind. Eng. Chem., 15 (2009) 524–528.

[5] R. Du, Y.Z. Peng, S.B. Cao, S.Y. Wang, C.C. Wu, Advanced nitrogen removal from wastewater by combining anammox with partial denitrification, Bioresour. Technol., 179 (2015) 497–504.

[6] N. Değermenci, O.N. Ata, E. Yildiz, Ammonia removal by air stripping in a semi-batch jet loop reactor, J. Ind. Eng. Chem., 18 (2012) 399–404.

[7] D. Ippersiel, M. Mondor, F. Lamarche, F. Tremblay, J. Dubreuil, L. Masse, Nitrogen potential recovery and concentration of ammonia from swine manure using electrodialysis coupled with air stripping, J. Environ. Manage., 95 (2012) S165–S169.

[8] H.M. Huang, L.Y. Huang, Q.R. Zhang, Y. Jiang, L. Ding, Chlorination decomposition of struvite and recycling of its product for the removal of ammonium-nitrogen from landfill leachate, Chemosphere, 136 (2015) 289–295.

[9] F. Nosratinia, M. Ghadiri, H. Ghahremani, Mathematical modeling and numerical simulation of ammonia removal from wastewaters using membrane contactors, J. Ind. Eng. Chem., 20 (2014) 2958–2963.

[10] T. Zhang, L.L. Ding, H.Q. Ren, X. Xiong, Ammonium nitrogen removal from coking wastewater by chemical precipitation recycle technology, Water Res., 43 (2009) 5209–5215.

[11] N. Yin, G. Yang, Z.X. Zhong, W.H. Xing, Separation of ammonium salts from coking wastewater with nanofiltration combined with diafiltration, Desalination, 268 (2011) 233–237.

[12] M.H. Liu, S.B. Wu, L. Chen, R.J. Dong, How substrate influences nitrogen transformations in tidal flow constructed wetlands treating high ammonium wastewater?, Ecol. Eng., 73 (2014) 478–486.

[13] X.G. Wang, S.Y. Lu, C.M. Gao, C. Feng, X.B. Xu, X. Bai, N.N. Gao, J.L. Yang, M.Z. Liu, L. Wu, Recovery of ammonium and phosphate from wastewater by wheat straw-based amphoteric adsorbent and reusing as a multifunctional slow-release compound fertilizer, Sustain. Chem. Eng., 4 (2016) 2068–2079.

[14] P.V. Haseena, K.S. Padmavathy, K.P. Rohit, G. Madhu, Adsorption of ammonium nitrogen from aqueous systems using chitosan-bentonite film composite, Procedia Technol., 24 (2016) 733–740.

[15] L. Zhao, Y.L. Li, S.D. Wang, X.Y. Wang, H.Q. Meng, S.H. Luo, Adsorption and transformation of ammonium ion in a loose pore geothermal reservoir: batch and column experiments, J. Contam. Hydrol., 192 (2016) 50–59.

[16] L. Lin, Z. Lei, L. Wang, X. Liu, Y. Zhang, C.L. Wan, D.J. Lee, J.H. Tay, Adsorption mechanisms of high-levels of ammonium onto natural and NaCl-modified zeolites, Sep. Purif. Technol., 103 (2013) 15–20.

[17] Z.M. Sun, X.S. Qu, G.F. Wang, S.L. Zheng, R.L. Frost, Removal characteristics of ammonium nitrogen from wastewater by modified Ca-bentonites, Appl. Clay Sci., 107 (2015) 46–51.

[18] K. Zare, H. Sadegh, R. Shahryari-Ghoshekandi, M. Asif, I. Tyagi, S. Agarwal, V.K. Gupta, Equilibrium and kinetic study of ammonium ion adsorption by Fe_3O_4 nanoparticles from aqueous solutions, J. Mol. Liq., 213 (2015) 345–350.

[19] K. Lu, X.L. Zhang, Y.L. Zhao, Z.L. Wu, Removal of color from textile dyeing wastewater by foam separation, J. Hazard. Mater., 182 (2010) 928–932.

[20] D. Dutta, D. Thakur, D. Bahadur, SnO_2 quantum dots decorated silica nanoparticles for fast removal of cationic dye (methylene blue) from wastewater, Chem. Eng. J., 281 (2015) 482–490.

[21] J.Z. Liu, J.B. Chen, Z.H. He, G.L. Zhang, Study on performance of concrete made from sewage sludge ceramsite, Open Mater. Sci. J., 5 (2011) 123–129.

[22] J. Mellor, L. Abebe, B. Ehdaie, R. Dillingham, J. Smith, Modeling the sustainability of a ceramic water filter intervention, Water Res., 49 (2014) 286–299.

[23] G.R. Xu, J.L. Zou, G.B. Li, Stabilization/solidification of heavy metals in sludge ceramsite and leachability affected by oxide substances, Environ. Sci. Technol., 43 (2009) 5902–5907.

[24] E. Furlani, G. Tonello, S. Maschio, E. Aneggi, D. Minichelli, S. Bruckner, Sintering and characterisation of ceramics containing paper sludge, glass cullet and different types of clayey materials, Ceram. Int., 37 (2011) 1293–1299.

[25] C. Wang, F.S. Zhang, Zeolite loaded ceramsite developed from construction and demolition waste, Mater. Lett., 93 (2013) 380–382.

[26] G.R. Xu, J.L. Zou, G.B. Li, Ceramsite made with water and wastewater sludge and its characteristics affected by SiO_2 and Al_2O_3, Environ. Sci. Technol., 42 (2008) 7417–7423.

[27] Y. Cheng, W.J. Fan, L. Guo, Coking wastewater treatment using a magnetic porous ceramsite carrier, Sep. Purif. Technol., 130 (2014) 167–172.

[28] Y. Zhang, F. He, S.B. Xia, L.W. Kong, D. Xu, Z.B. Wu, Adsorption of sediment phosphorus by porous ceramic filter media coated with nano-titanium dioxide film, Ecol. Eng., 64 (2014) 186–192.

[29] S.J. Kang, K. Egashira, A. Yoshida, Transformation of a low-grade Korean natural zeolite to high cation exchanger by hydrothermal reaction with or without fusion with sodium hydroxide, Appl. Clay Sci., 13 (1998) 117–135.

[30] T.P. Li, T.T. Sun, B.A. Tallal, D.X. Li, Photocatalytic degradation of methylene blue in aqueous solution using ceramsite coated with micro-Cu_2O under visible-light irradiation, Korean J. Chem. Eng., 34 (2017) 1199–1207.

[31] T.P. Li, T.T. Sun, D.X. Li, Removal of methylene blue from aqueous solution by ceramsite filter media combined with high temperature calcination for regeneration, Desal. Wat. Treat., 59 (2017) 220–229.

[32] T.P. Li, T.T. Sun, B.A. Tallal, D.X. Li, X.L. Lin, Y.L. Li, Preparation and physical properties of ceramsite filter media for water treatment obtained from municipal solid wastes, J. Donghua Univ. (Eng. Ed.), 34 (2017) 39–44.

[33] T.P. Li, T.T. Sun, D.X. Li, Preparation, sintering behavior and expansion performance of ceramsite filter media from dewatered sewage sludge, coal fly ash and river sediment, J. Mater. Cycles Waste Manage., (2016). doi: 10.1007/s10163-016-0547-3.

[34] G.R. Xu, J.L. Zou, G.B. Li, Ceramsite obtained from water and wastewater sludge and its characteristics affected by $(Fe_2O_3+CaO+MgO)/(SiO_2+Al_2O_3)$, Water Res., 43 (2009) 2885–2893.

[35] Y.Q. Zhao, Q.Y. Yue, R.B. Li, M. Yue, S.X. Han, B.Y. Gao, Q. Li, H. Yu, Research on sludge-fly ash ceramic particles (SFCP) for synthetic and municipal wastewater treatment in biological aerated filter (BAF), Bioresour. Technol., 100 (2009) 4955–4962.

[36] Y.F. Wang, F. Lin, W.Q. Pang, Ammonium exchange in aqueous solution using Chinese natural clinoptilolite and modified zeolite, J. Hazard. Mater., 142 (2007) 160–164.

[37] A. Alshameri, A. Ibrahim, A.M. Assabri, X.R. Lei, H.Q. Wang, C.J. Yan, The investigation into the ammonium removal performance of Yemeni natural zeolite: modification, ion exchange mechanism, and thermodynamics, Powder Technol., 258 (2014) 20–31.

[38] F. López-Linares, L. Carbognani, C.S. Stull, P. Pereira-Almao, Adsorption kinetics of anilines on macroporous kaolin, Energy Fuels, 22 (2008) 2188–2194.

[39] M. Li, H.T. Kao, Z.S. Wu, J.M. Tan, Study on preparation and thermal property of binary fatty acid and the binary fatty acids/diatomite composite phase change materials, Appl. Energy, 88 (2011) 1606–1612.

[40] H.T. He, P. Zhao, Q.Y. Yue, B.Y. Gao, D.T. Yue, Q. Li, A novel polynary fatty acid/sludge ceramsite composite phase change materials and its applications in building energy conservation, Renew. Energy, 76 (2015) 45–52.

[41] Z.M. Feng, T. Sun, A novel selective hybrid cation exchanger for low-concentration ammonia nitrogen removal from natural water and secondary wastewater, Chem. Eng. J., 281 (2015) 295–302.

[42] G.D. Ji, Y. Zhou, J.J. Tong, Nitrogen and phosphorus adsorption behavior of ceramsite material made from coal ash and metallic iron, Environ. Eng. Sci., 27 (2010) 871–878.

[43] L. Yang, J. Wei, Z.Y. Liu, J.L. Wang, D.T. Wang, Material prepared from drinking waterworks sludge as adsorbent for ammonium removal from wastewater, Appl. Surf. Sci., 330 (2015) 228–236.

[44] Y.X. Zhao, Y.N. Yang, S.J. Yang, Q.H. Wang, C.P. Feng, Z.Y. Zhang, Adsorption of high ammonium nitrogen from wastewater using a novel ceramic adsorbent and the evaluation of the ammonium-adsorbed-ceramic as fertilizer, J. Colloid Interface Sci., 393 (2013) 264–270.

[45] X.S. Yi, G.S. Li, Y.Y. Yin, Pedotransfer functions for estimating soil bulk density: a case study in the three-river headwater region of Qinghai province, China, Pedosphere, 26 (2016) 362–373.

[46] U.R. Nd, S.C. Baxter, Y.Z. Chen, R.N. Shah, K.D. Shimizu, Characterization of molecularly imprinted polymers with the Langmuir-Freundlich isotherm, Anal. Chem., 73 (2001) 4584–4591.

[47] H.M. Huang, X.M. Xiao, B. Yan, L.P. Yang, Ammonium removal from aqueous solutions by using natural Chinese (Chende) zeolite as adsorbent, J. Hazard. Mater., 175 (2010) 247–252.

[48] X.T. Sun, Q. Li, L.R. Yang, H.Z. Liu, Removal of chromium (VI) from wastewater using weakly and strongly basic magnetic adsorptions: adsorption/desorption property and mechanism comparative studies, RSC Adv., 6 (2016) 18471–18482.

[49] Y. Wimalasiri, M. Mossad, L. Zou, Thermodynamics and kinetics of adsorption of ammonium ions by graphene laminate electrodes in capacitive deionization, Desalination, 357 (2015) 178–188.

[50] A. Zohreh, Y. Habibollah, B. Nader, Batch and column adsorption of reactive red 198 from textile industry effluent by microporous activated carbon developed from walnut shells, Waste Biomass Valorization, 7 (2016) 1255–1270.

[51] Y. Yu, Y.Y. Zhang, Z.H. Wang, M.Q. Qiu, Adsorption of water-soluble dyes onto modified resin, Chemosphere, 54 (2004) 425–430.

[52] L. Zhou, J.C. Huang, B.Z. He, F.A. Zhang, H.B. Li, Peach gum for efficient removal of methylene blue and methyl violet dyes from aqueous solution, Carbohydr. Polym., 101 (2014) 574–581.

[53] Q. Zhou, Q. Gao, W.J. Luo, C.J. Yan, Z.N. Ji, P. Duan, One-step synthesis of amino-functionalized attapulgite clay nanoparticles adsorbent by hydrothermal carbonization of chitosan for removal of methylene blue from wastewater, Colloids Surf., 470 (2015) 248–257.

[54] H.M. Huang, L.P. Yang, Q. Xue, J.H. Liu, L. Hou, L. Ding, Removal of ammonium from swine wastewater by zeolite combined with chlorination for regeneration, J. Environ. Manage., 160 (2015) 333–341.

[55] M. Li, C. Feng, Z. Zhang, Simultaneous regeneration of zeolites and removal of ammonia using an electrochemical method, Microporous Mesoporous Mater., 127 (2010) 161–166.